Trans. Phenom. Nano Micro Scales, 1(1): 26-36, Winter - Spring 2013
DOI: 10.7508/tpnms.2013.01.003

ORIGINAL RESEARCH PAPER

Numerical Study of Mixed Convection of Nanofluid in a Concentric Annulus with Rotating Inner Cylinder

G. A. Sheikhzadeh [1], H. Teimouri [1,*], M. Mahmoodi [1, 2]
[1] *Department of Mechanical Engineering, University of Kashan, Kashan, Iran*
[2] *Department of Mechanical Engineering, Amirkabir University of Technology, Tehran, Iran*

Abstract

In this work, the steady and laminar mixed convection of nanofluid in horizontal concentric annulus with rotating inner cylinder is investigated numerically. The inner and outer cylinders are kept at constant temperature T_i and T_o respectively, where $T_i>T_o$. The annular space is filled with Alumina-water nanofluid. The governing equations with the corresponded boundary conditions in the polar coordinate are discretized using the finite volume method where pressure-velocity coupling is done by the SIMPLER algorithm. Numerical results have been obtained for Rayleigh number ranging from 10^2 to 10^5, Reynolds number from 1 to 300 and nanoparticles volume fraction from 0.01 to 0.06. The effects of the Reynolds and Rayleigh numbers, average diameter of nanoparticles and the volume fraction of the nanoparticles on the fluid flow and heat transfer inside the annuli are investigated. According to the results, the average Nusselt number decreases with increasing the Reynolds number. However, the average Nusselt number increases by increasing the Rayleigh number. Moreover, the maximum average Nusselt number occurs for an optimal nanoparticle volume fraction except situations that heat conduction predominates over the heat convection. In these conditions the average Nusselt number is close to unity.

Keywords: *Concentric Annulus;Mixed Convection; Nanofluid; Finite Volume Method; Rotating Inner Cylinder*

1. Introduction

The problem of mixed convection in annulus between two rotating cylinders is noteworthy because of its wide applications. Some applications are methods for improvement of crystal formation in technological applications [1,2] food processing [3, 4], and journal bearing. The increase of generation of heat in industrial devices with decrease of their size increases need for higher heat transfer rate in minimum space. In spite of all of the advances in enhancement of heat transfer, the low thermal conductivity of the traditional coolants is a great limitation in this way. One of the methods for increase the heat transfer is use of nanoparticles in the base fluid. The existence of the nanoparticles increases the viscosity which is an undesirable effect and reduces the rate of heat transfer. Based on these effects of nanoparticles, they can reduces or increases the rate of heat transfer based on the geometry and boundary conditions of the problem, type, size, shape, and volume fraction of the nanoparticles. Therefore when the nanofluid is used its effect on heat transfer must be investigated firstly.

In continue some of works done on mixed convection in annuluses with rotating inner cylinder

[*]Corresponding author
Email Address: hamidtmr@gmail.com

Nomenclature

p	Pressure(N m^{-2})	θ	Angle
P	Dimensionless pressure	Θ	Dimensionless temperature
Pr	Prandtl number	μ	Dynamic viscosity ($N\ s\ m^{-2}$)
r	Radial coordinate(m)	ν	Kinematic viscosity (m^2 s^{-1})
R	Dimensionless radial distance	ρ	Density ($kg\ m^{-3}$)
RR	Radius ratio	φ_p	Nanoparticle volume fraction
R'	Dimensionless position $\frac{r-r_i}{r_o-r_i}$	ψ	Stream function ($m^2 s^{-1}$)
Ra	Rayleigh number	Ψ	Dimensionless stream function
Re	Reynolds number	ω	Angular velocity(rad s^{-1})
T	Temperature (K)		
u, v	Velocity components(m s^{-1})		**Subscripts**
U, V	Dimensionless velocity components	eff.	Effective
		f_0	Fluid
	Greek symbols	i	Inner
α	Thermal diffusivity (m^2 s^{-1})	nf	Nanofluid
β	Thermal expansion coefficient (K^{-1})	o	Outer

are reviewed. These works have been done for rotating Reynolds number lower than 2000 which the flow becomes two dimensional and laminar. As early as 1992, Lee [5] studied numerically laminar natural convection of air in eccentric annulus with rotating inner cylinders. He observed that in a constant Rayleigh number the average Nusselt number decreases with increase in rotation velocity of inner cylinder. Natural convection of nanofluids in a concentric annulus was firstly studied numerically by Abu-Nada et al. [6]. They used Brinkman [7] and Hamilton-Crosser [8] models for viscosity and thermal conductivity of the nanofluid, respectively. They observed enhanced heat transfer using nanofluid at low Rayleigh numbers. Abu-Nada [9,10] investigated effects of different viscosity and thermal conductivity models for nanofluid on natural convection in concentric annuluses. Izadi et al. [11] conducted a numerical study on developing laminar forced convection of Al_2O_3-water nanofluid in an annulus. They used Masoumi et al. [12] and Chon et al. [13] correlations for prediction of viscosity and thermal conductivity of the nanofluid, respectively.

Their results showed that, in general, convective heat transfer coefficient increases with nanoparticle concentration.

Base on the knowledge of the authors effect of nanoparticles on flow pattern and mixed convection in annulus between two concentric cylinders with rotating inner cylinder has not been investigated in literature. In the present work this problem is investigated.

2. Problem definition

Figure 1 shows the geometry of present problem. Inner cylinder with radius of r_i and the outer cylinder with radius of r_o are kept at temperatures of T_i and T_o, respectively. The inner warmer cylinder rotates with the angular velocity of ω in counterclockwise direction. The annulus has infinite length. The annulus is filled with Al_2O_3-water nanofluid. According to ref. [14] for the Reynolds number lower than 2000 that the Taylor vortices are not formed the flow is two dimensional. In the present problem the natural convection is due to the temperature difference and gravity, while the forced convection is due to the rotation of inner cylinder. In the present work the effects of nanoparticles with different average diameters and volume fraction on the flow pattern and heat transfer are investigated. Also the effects of boundary conditions such as angular velocity of inner cylinder (Reynolds number) and temperature difference of two cylinders (Rayleigh number) are considered.

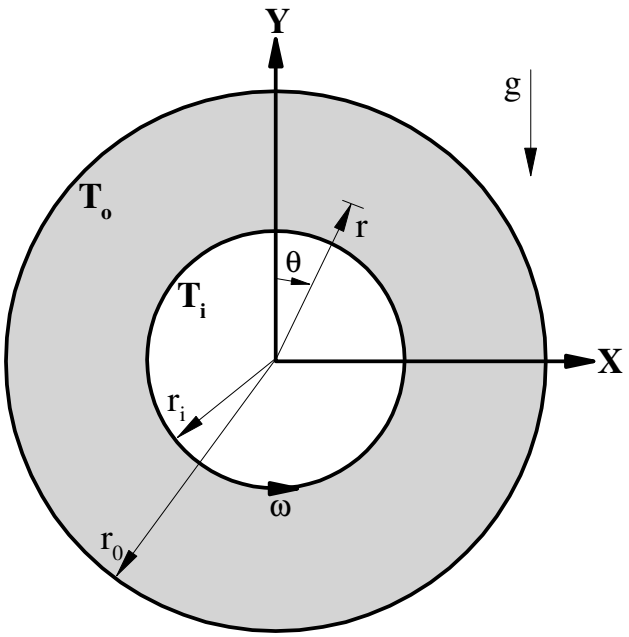


Fig. 1. Geometry of the problem and the boundary conditions

3. Mathematical modeling

The thermophysical properties of the nanofluid are considered to be constant with the exception of density in the buoyancy term in the momentum equation which varies according to the Boussinesq approximation. The nanoparticles are assumed to be uniform in shape and size. Moreover, the base fluid and the nanoparticles are assumed to be in thermal equilibrium. There is not any slip between the water and the nanoparticles. With the assumption of Newtonian fluid, steady state and incompressible flow, the governing equations in polar system coordinates are as follows:

Continuity:

$$\frac{\partial v}{\partial r}+\frac{v}{r}+\frac{1}{r}\frac{\partial u}{\partial \theta}=0 \tag{1}$$

Momentum equation in r direction:

$$\rho_{nf}\left(v\frac{\partial v}{\partial r}+\frac{u}{r}\frac{\partial v}{\partial \theta}-\frac{u^2}{r}\right)=-\frac{\partial p}{\partial r}+\mu_{nf}\left(\frac{\partial^2 v}{\partial r^2}+\frac{1}{r}\frac{\partial v}{\partial r}-\frac{v}{r^2}+\frac{1}{r^2}\frac{\partial^2 v}{\partial \theta^2}-\frac{2}{r^2}\frac{\partial u}{\partial \theta}\right)+f_r \tag{2}$$

Momentum equation in θ direction:

$$\rho_{nf}\left(v\frac{\partial u}{\partial r}+\frac{u}{r}\frac{\partial u}{\partial \theta}+\frac{uv}{r}\right)=-\frac{1}{r}\frac{\partial p}{\partial \theta}+\mu_{nf}\left(\frac{\partial^2 u}{\partial r^2}+\frac{1}{r}\frac{\partial u}{\partial r}-\frac{u}{r^2}+\frac{1}{r^2}\frac{\partial^2 u}{\partial \theta^2}+\frac{2}{r^2}\frac{\partial v}{\partial \theta}\right)+f_\theta \tag{3}$$

Energy equation:

$$v\frac{\partial T}{\partial r}+\frac{u}{r}\frac{\partial T}{\partial \theta}=\alpha_{nf}\left(\frac{\partial^2 T}{\partial r^2}+\frac{1}{r}\frac{\partial T}{\partial r}+\frac{1}{r^2}\frac{\partial^2 T}{\partial \theta^2}\right) \tag{4}$$

Where u and v are velocity components in radial and tangential direction, g is gravitational acceleration, μ, ρ, β, and α are viscosity, density, thermal expansion coefficient and thermal diffusivity coefficient, respectively. f_r and f_θ are components of volumetric forces in radial and tangential directions as follows:

$$f_r=(\rho\beta)_{nf}g(T-T_o)\cos\theta \qquad f_\theta=-(\rho\beta)_{nf}g(T-T_o)\sin\theta \tag{5}$$

The boundary conditions are:

$$v=0,\quad u=r_i\omega,\quad T=T_i \ \ at \ \ r=r_i \qquad v=0,\quad u=0,\quad T=T_o \ \ at \ \ r=r_o \tag{6}$$

The following dimensionless parameters are considered in the problem [15, 16]:

$$R=\frac{r}{l}\qquad \Theta=\frac{T-T_o}{T_i-T_o}\qquad V=\frac{v}{r_i\omega}$$

$$U=\frac{u}{r_i\omega}\qquad P=\frac{p}{\rho {r_i}^2\omega^2} \tag{7}$$

$$\Psi=\frac{\psi}{r_i\omega l}\qquad E=\frac{e}{l} \tag{8}$$

where l is radius differences of inner and outer cylinders and is equal to (r_o – r_i). With the above parameters the governing equations are converted in non-dimensional form:

Continuity:

$$\frac{\partial V}{\partial R}+\frac{V}{R}+\frac{1}{R}\frac{\partial U}{\partial \theta}=0 \tag{9}$$

Momentum equation in *r* direction:

$$V\frac{\partial V}{\partial R}+\frac{U}{R}\frac{\partial V}{\partial \theta}-\frac{U^2}{R} = -\frac{\rho_f}{\rho_{nf}}\frac{\partial P}{\partial R} + \frac{\nu_{nf}}{\nu_f}\frac{1}{Re}\left(\frac{\partial^2 V}{\partial R^2}+\frac{1}{R}\frac{\partial V}{\partial R}-\frac{V}{R^2} + \frac{1}{R^2}\frac{\partial^2 V}{\partial \theta^2}-\frac{2}{R^2}\frac{\partial U}{\partial \theta}\right) + \frac{\beta_{nf}}{\beta_f}\frac{Ra}{PrRe^2}\Theta\cos\theta \quad (10)$$

Momentum equation in θ direction:

$$V\frac{\partial U}{\partial R}+\frac{U}{R}\frac{\partial U}{\partial \theta}+\frac{UV}{R} = -\frac{\rho_f}{\rho_{nf}}\frac{1}{R}\frac{\partial P}{\partial \theta} + \frac{\nu_{nf}}{\nu_f}\frac{1}{Re}\left(\frac{\partial^2 U}{\partial R^2}+\frac{1}{R}\frac{\partial U}{\partial R}-\frac{U}{R^2} + \frac{1}{R^2}\frac{\partial^2 U}{\partial \theta^2}+\frac{2}{R^2}\frac{\partial V}{\partial \theta}\right) - \frac{\beta_{nf}}{\beta_f}\frac{Ra}{PrRe^2}\Theta\sin\theta \quad (11)$$

Energy equation:

$$V\frac{\partial \Theta}{\partial R}+\frac{U}{R}\frac{\partial \Theta}{\partial \theta} = \frac{\alpha_{nf}}{\alpha_f}\frac{1}{RePr}\left(\frac{\partial^2 \Theta}{\partial R^2}+\frac{1}{R}\frac{\partial \Theta}{\partial R} + \frac{1}{R^2}\frac{\partial^2 \Theta}{\partial \theta^2}\right) \quad (12)$$

where *Ra*, *Pr*, and *Re* are Rayleigh, Prandtl, and Reynolds number and are defined as follows:

$$Ra=\frac{g\beta_f(T_i-T_o)l^3}{\alpha_f\nu_f}, \qquad Pr=\frac{\nu_f}{\alpha_f}, \qquad Re=\frac{r_i\omega l}{\nu_f} \quad (13)$$

Also the boundary conditions in dimensionless form are:

$$V=0, \quad U=1, \quad \Theta=1 \ \ at \ \ R=R_i$$
$$V=0, \quad U=0, \quad \Theta=0 \ \ at \ \ R=R_o \quad (14)$$

The density, heat capacity, and thermal expansion coefficient of the nanofluid are:

$$\rho_{eff}=(1-\varphi_p)\rho_f+\varphi_p\rho_p \quad (15)$$

$$c_{eff}=\frac{(1-\varphi_p)\rho_f c_f+\varphi_p\rho_p c_p}{\rho_{eff}} \quad (16)$$

$$\beta_{eff}=\frac{(1-\varphi_p)(\rho\beta)_f+\varphi_p(\rho\beta)_p}{\rho_{eff}} \quad (17)$$

Viscosity and thermal conductivity of nanofluid is calculated with the assumption of thermal equilibrium between base fluid and nanoparticles and uniform shape of the nanoparticles. The viscosity of Al_2O_3-water nanofluid with average diameters of 13, 28, and 36 mm is calculated by [17-19]:

$$\mu_{eff}=(1+39.11\varphi_p+533.9{\varphi_p}^2)\mu_f \quad d_p=13\ nm. \quad (18)$$

$$\mu_{eff}=(1+7.3\varphi_p+123{\varphi_p}^2)\mu_f \quad d_p=28\ nm. \quad (19)$$

$$\mu_{eff}=(1+0.025\varphi_p+0.015{\varphi_p}^2)\mu_f \quad d_p=36\ nm. \quad (20)$$

In (20) φ_p is in percentage. Thermal conductivity of Al_2O_3-water nanofluid is calculated according to the model proposed by Khanafer and Vafai [20]:

$$\left(\frac{k_{eff}}{k_f}\right)_{Al_2O_3} = 0.9843 + 0.398{\varphi_p}^{0.7383}\left(\frac{1}{d_p(nm)}\right)^{0.2246}\left(\frac{\mu_{eff}(T)}{\mu_f(T)}\right)^{0.0235} -3.9517\frac{\varphi_p}{T}+34.034\frac{{\varphi_p}^2}{T^3}+32.509\frac{\varphi_p}{T^2} \quad (21)$$

$0\le\varphi_p\le 10\%;$
$11nm\le d\le 150nm;$
$20°C\le T\le 70°C$

Where φ_p is in percentage, *T* is in Celsius, and d_p is in nm. The viscosity of water in different temperatures is obtained by:

$$\mu_f(T)=2.414\times10^{-5}\times10^{247.8/(T-140)} \quad (22)$$

Where *T* is in Kelvin. The thermophysical properties of water and Al_2O_3 at 293 K are presented in Table 1.

Table 1
Thermophysical properties of water and Al_2O_3

	$\beta\times10^5$ (1/K)	k (W/m K)	c_p (J/kg K)	ρ (kg/m^3)	T (K)	Pr
Water [21]	21	0.59	4182	998.2	293	7.07
Al_2O_3 [9]	25	0.85	765	3970	293	–

The local Nusselt numbers on the inner and outer cylinders are calculated by the following equations [15, 22, 23]:

$$Nu_i = -r_i ln\left(\frac{r_o}{r_i}\right)\frac{k_{nf}}{k_f}\frac{1}{T_i - T_o}\frac{\partial T}{\partial r}\bigg|_{r=r_i} \quad (23)$$

$$Nu_o = -r_o ln\left(\frac{r_o}{r_i}\right)\frac{k_{nf}}{k_f}\frac{1}{T_i - T_o}\frac{\partial T}{\partial r}\bigg|_{r=r_o} \quad (24)$$

The average Nusselt number on the inner cylinder is calculated by:

$$\overline{Nu_i} = \frac{1}{2\pi}\int_0^{2\pi} Nu_i(\theta)d\theta \quad (25)$$

Also the Nusselt number based on the dimensionless parameters is:

$$Nu_i = -R_i ln\left(\frac{R_o}{R_i}\right)\frac{k_{nf}}{k_f}\frac{\partial \Theta}{\partial R}\bigg|_{R=R_i} \quad (26)$$

The streamfunction in polar coordinates is as follows:

$$v = \frac{1}{r}\frac{\partial \psi}{\partial \theta}, \qquad u = -\frac{\partial \psi}{\partial r} \quad (27)$$

4. Numerical implementation

The governing equations with the respective boundary conditions are discretized using the finite volume method. As shown in Fig. 2 a non-uniform grid is generated, then the governing equations are discretized on the grid points. The diffusion terms are discretized using a central difference scheme, while a hybrid scheme, which is a combination of central difference and upwind schemes, is used to discretize the convective terms. The velocity and pressure fields are coupled according to the SIMPLER algorithm based on a staggered grid. The set of algebraic equations are solved iteratively using TDMA method.

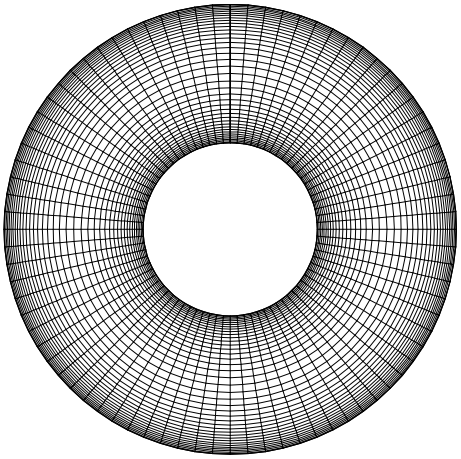


Fig. 2. Non-uniform grid for the computational domain

Different grid sizes are examined to ensure grid independence results. The tested grids and the obtained average Nusselt numbers are shown in Table 2. The results are obtained for air with Pr = 0.7, Re = 257 and Ra = 10^5. The outer cylinder to inner cylinder diameter ratio is 2.6. Figure 3 shows variation of tangential velocity at θ = 90 for different grid sizes. According to the Fig. 3 and Table 2, an 81×41 grid is sufficiently fine. It should be noted that 81 points are in tangential direction while 41 grid points are in radial direction.

Table 2
average Nusselt number for different grid sizes

	101×51	81×41	61×31	41×21
$\overline{Nu}$	3.518	3.514	3.505	3.487

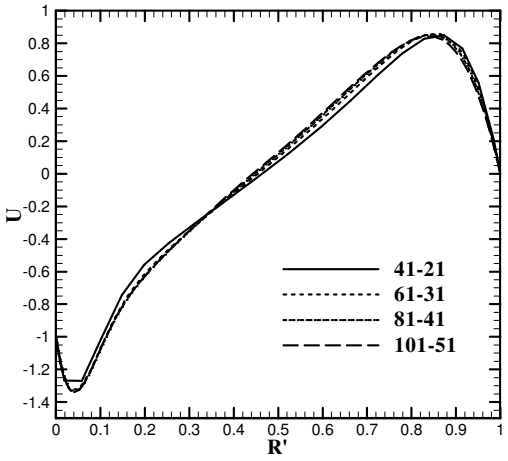


Fig. 3. variation of tangential velocity at θ = 90 for different grid sizes

For validation of the results, the obtained results in the present study are compared with results of other researchers. At the first step natural convection of air in a cylindrical annulus with constant temperature walls at $Ra = 5\times10^4$ and diameter ratio of 2.6 is considered. The obtained results are compared with those of Kuehn and Goldstein [22] in Figs. 4 and 5.

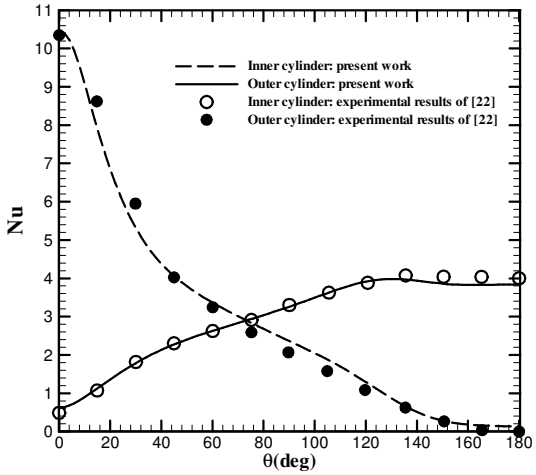


Fig. 4. Comparison of the local Nusselt number for two concentric cylinders obtained in the present study with those of Kuehn and Goldstein [22]

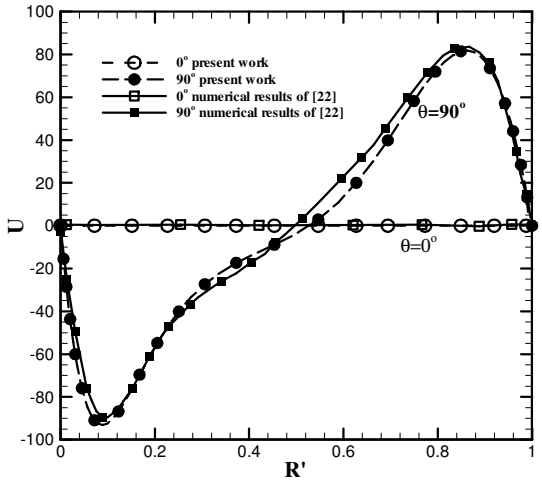


Fig. 5. Comparison of the tangential velocity for two concentric cylinders obtained in the present study with those of Kuehn and Goldstein [22]

Another test case is mixed convection in concentric annulus with rotating inner cylinder. The results are compared with those of Char and Hsu [16] and Lee [5] in Figs. 6 and 7. In Fig. 6 the *Pr*, *Ra*, and *Re* are 0.7, 10^5 and 119, respectively. In Fig. 7 the *Pr* and *Ra* are 0.7 and 10^5 respectively. As can be seen in the figures a good agreement exists between the results. The minor difference is due to difference in used numerical techniques and accuracy of discretization.

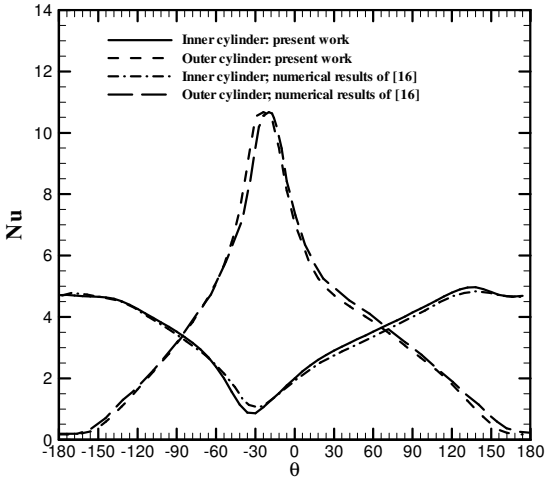


Fig. 6. Comparison of the local Nusselt number for two concentric cylinders with rotating inner cylinder obtained in the present study with those of Char and Hsu [16]

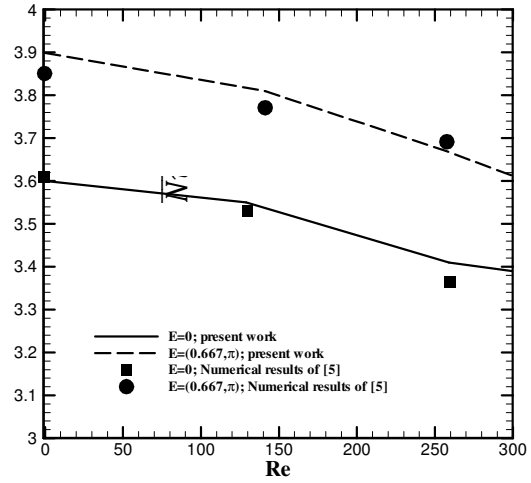


Fig. 7. Comparison of the average Nusselt number for two concentric cylinders with rotating inner cylinder obtained in the present study with those of Lee [5]

5. Results and discussions

5.1. Effect of Reynolds number on flow pattern and temperature distribution

In this section effect of Reynolds number on fluid flow and heat transfer of Al_2O_3-water nanofluid in the annulus is considered. The diameter ratio of annulus is 2.6, the Rayleigh number is 10^4, the average temperature of the walls is 293 K and the volume fraction of the nanoparticles is varying from 0 to 0.06. The results are obtained for *Re* = 1, 25, 100, and 300. Therefore the Richardson number which evaluate the

strength of natural convection compared to the forced convection is Ri = 1414.42, 2.26, 0.14, and 0.016.

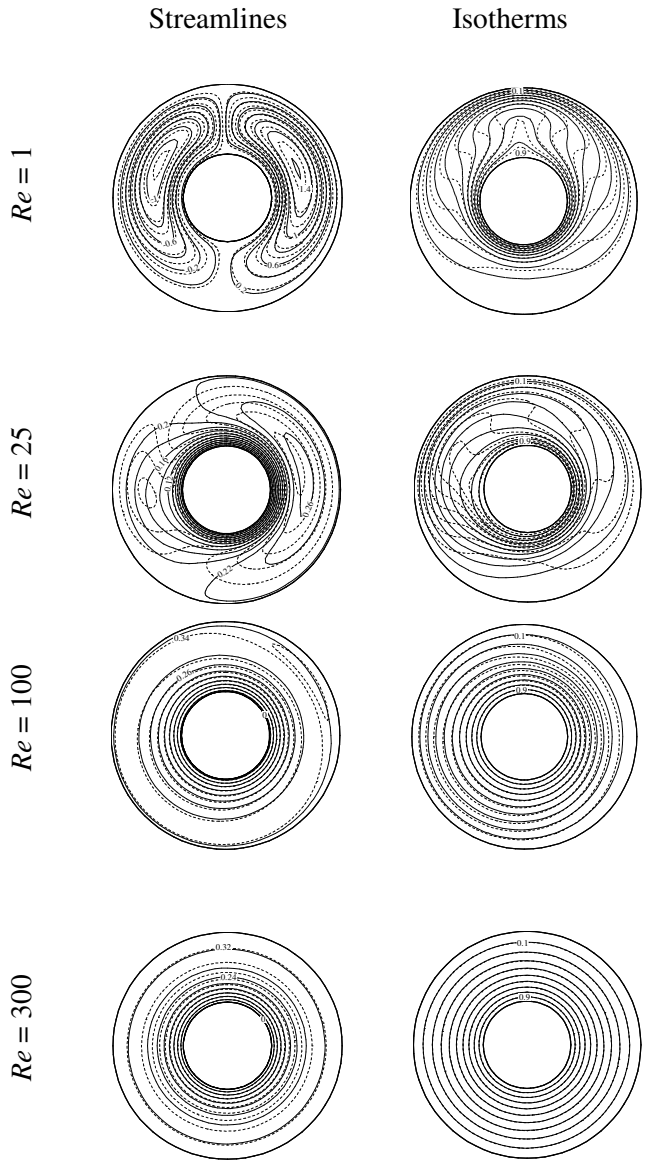


Fig. 8. Streamlines and isotherms at Ra = 104 and different Reynolds numbers for nanofluid with φ_p = 0.06 (solid line) and pure fluid (dashed line)

Figure 8 shows the streamlines and isotherms for nanofluid and base fluid. As can be seen from the streamlines at Re = 1 the rotation of the inner cylinder has a minor effect and two vortices are formed in side of the inner cylinder. These vortices are approximately symmetric. The fluid is heated at the vicinity of the inner cylinder and moves upward. Then blocked by the upper region of the outer cylinder and is cooled when moves downward along it. At this conditions the Richardson number is equal to 1414.14 and the natural convection is dominated the heat transfer. Also it is observed from Table 3 that the maximum value of stream function decreases with increase in φ_p.

Table 3
Minimum and maximum values of stream function for different values of Reynolds number

Re	$\varphi = 0.06$		$\varphi = 0$	
	ψ_{max}	ψ_{min}	ψ_{max}	ψ_{min}
1	1.414	-1.115	1.891	-1.633
25	0.266	0	0.226	0
100	0.340	0	0.343	0
300	0.328	0	0.359	0

With increase in the Reynolds number the right and left hand side vortices increases and decreases in size, respectively. Also the isotherms are condensed at the vicinity of the inner cylinder. The thermal plume is shifted to the left in the direction of rotation of the cylinder. With further increase in the Reynolds number the weak vortex formed by natural convection effect disappears. At Re = 100 and 300 the heat transfer occurs mainly through conduction and the average Nusselt number is close to unity and therefore the Nusselt number increases by increase in φ_p. In contrast with Re = 100 that for φ_p = 0.06 the streamfunction has a little increase compared to the base fluid, at Re = 300 for φ_p = 0.06 stream function decreases compared to the base fluid.

The local Nusselt numbers along the inner and outer cylinders at different Reynolds numbers are presented in Fig. 9 and Fig. 10, respectively. At Re = 1 the Nusselt number is approximately symmetric. Minimum heat transfer on the inner cylinder occurs on the location of separation of the plume, while its maximum value is on the lower portion of the cylinder. A reverse Nusselt number distribution is observed along the outer cylinder. With increase in Re minimum value of Nusselt number shifts the left side and variation of the Nusselt number decreases. At Re = 100 and 300 that heat transfer occurs mainly through conduction the Nusselt number is close to unity.

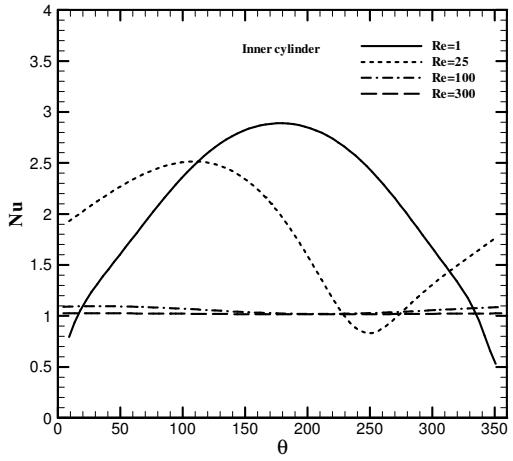


Fig. 9. Nusselt number distribution along the inner cylinder for different Reynolds numbers

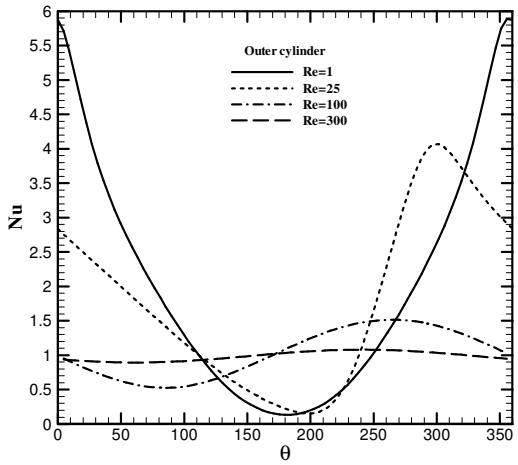


Fig. 10. Nusselt number distribution along the outer cylinder for different Reynolds numbers

Figure 11 shows variations of average Nusselt number with volume fraction of the nanoparticles at different Reynolds numbers. It is observed that by increase in Reynolds number the Nusselt number decreases and reaches to unity. This behaviour is according to the results of ref.[16]. At Re = 1 and 25 with increase in φ_p from 0 to 0.01 the Nusselt number increases while with further increase in φ_p it decreases. At Re = 100 and 300 with increase in φ_p the Nusselt number show an increasing trend.

5.2. Effect of Rayleigh number on fluid flow and heat transfer in the annulus

In this section effects of variation of Rayleigh number on fluid flow and heat transfer in the concentric annulus are investigated. The results are obtained for diameter ratio of 2.6, Re = 25 and average temperature of 293 K. the Rayleigh number is varying from 10^2 to 10^5.

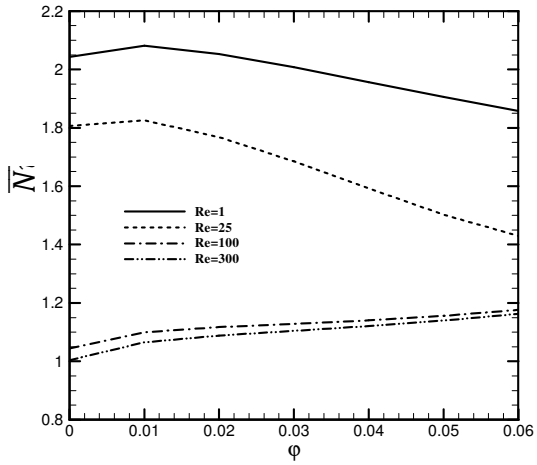


Fig. 11. Average Nusselt number versus φ_p at $Ra = 10^4$ and different values of Re

The streamlines and isotherms are shown in Fig. 12. As can be seen from the figure at $Ra = 10^2$ and 10^3 there is no vortices in the annulus. At these Rayleigh number the heat transfer occurs through conduction and therefore the increase in φ_p motivates the Nusselt number to increases. At $Ra = 10^4$ a thermal plume is formed. By increase in Rayleigh number the plume moves to the upper region of the outer cylinder and the strength of the vortices increases. At $Ra = 10^5$ the isotherms are condensed which is characteristics of temperature gradient and motivates the Nusselt number to increase. At this Rayleigh number the existence of the nanoparticles reduces the strength of the vortices.

In Fig. 13 the average Nusselt numbers versus the volume fraction of the nanoparticles are illustrated. At $Ra = 10^2$ and 10^3, which is conduction dominated regime, the Nusselt number is close to unity. At these Rayleigh numbers with increase in φ_p an increasing trend in Nusselt number is observed. At $Ra = 10^4$ a significant increase in Nusselt number in comparison with lower Rayleigh numbers is observed. It is because of formation of thermal plume at this Rayleigh number. At $Ra = 10^4$ and 10^5 the Nusselt number increases with increase in φ_p from 0 to 0.01. Further increase in φ_p motivates the Nusselt number to decrease.

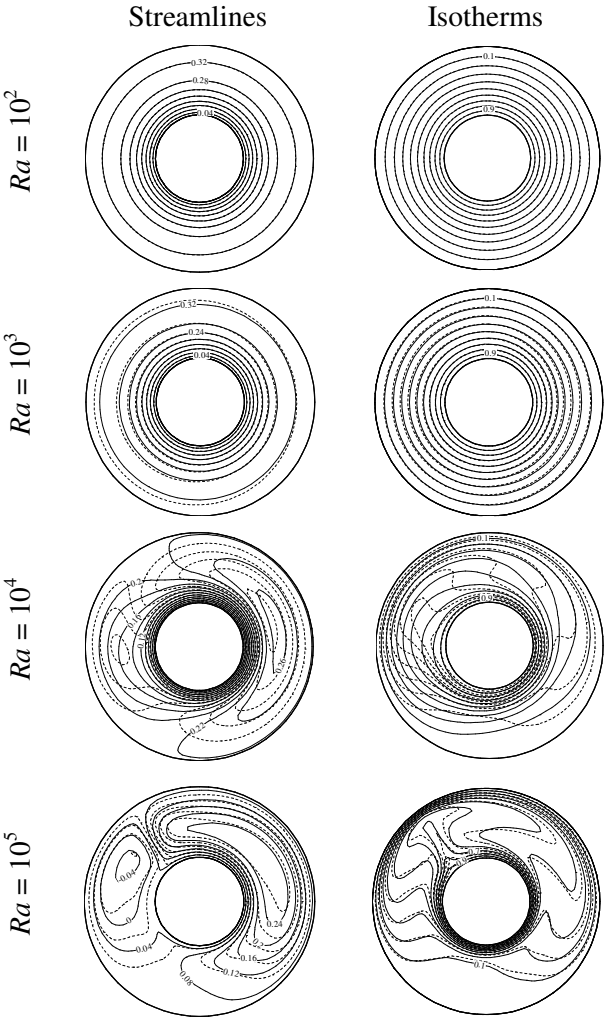


Fig. 12. Streamlines and isotherms at Re = 25 and different Rayleigh numbers for nanofluid with φ_p = 0.06 (solid line) and pure fluid (dashed line)

5.3. Effect of average diameter of nanoparticles on the average Nusselt number:

The average diameter of the nanoparticles due to their effect on effective viscosity and thermal conductivity of the nanofluid has a great effect on average Nusselt number. Figure 14 depicted average Nusselt number versus volume fraction of the nanoparticles for different values of nanoparticles diameter at Re = 25 and $Ra = 10^4$.

As can be seen from the figure the average Nusselt number increases with increase in nanoparticles diameter. For d_p = 13 nm the increase in $\varphi_p$motivates the Nusselt number to decreases. The nanofluid with d_p=36 nm has the highest effect on heat transfer enhancement.

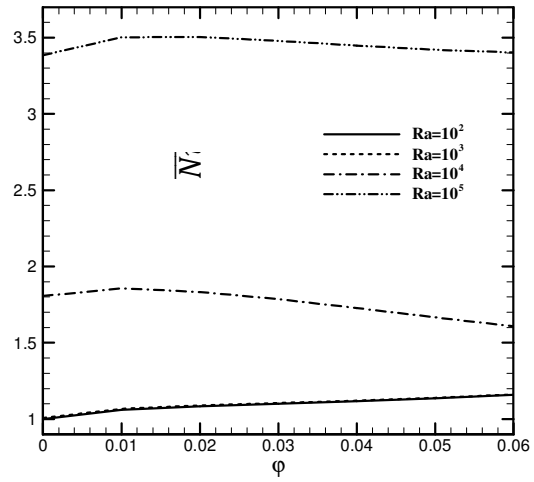


Fig. 13. Average Nusselt numbers versus volume fraction of the nanoparticles at Re = 25 and different Rayleigh numbers

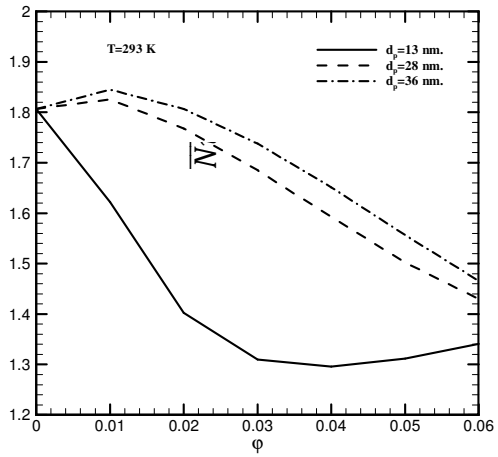


Fig. 14. Average Nusselt number versus volume fraction of the nanoparticles for different values of nanoparticles diameter at Re = 25 and $Ra = 10^4$

6. Conclusion

Mixed convection of Al_2O_3-water nanofluid in a concentric cylindrical annulus with rotating inner cylinder was investigated numerically. Effects of some pertinent parameters such as Reynolds number, Rayleigh number, volume fraction of the nanoparticles, and average diameter of the nanoparticles on fluid flow and heat transfer were considered. The main findings of the paper are stated below:

1- The increase in Reynolds number reduces the Nusselt number. At high Reynolds numbers and low Richardson numbers the heat transfer occurs mainly through conduction and the Nusselt number closes to unity.

2- At all Rayleigh numbers with increase in Reynolds number the local Nusselt number decreases and closes to unity.

3- At low Reynolds number and high Richardson numbers, which is a convection dominated regime, with increase in volume fraction of the nanoparticles the Nusselt number firstly increases and then decreases. Therefore an optimum value of φ_p exists in which maximum heat transfer occurs. At high Reynolds numbers and low Richardson numbers (conduction dominated regime) with increase in volume fraction of the nanoparticles the Nusselt number increases.

References

[1] H.Q. Yang, K.T. Yang and J.R. Lloyd, Rotational effects on natural convection in a horizontal cylinder, AIChE Journal 34 (1988) 1627-1633.

[2] H.Q. Yang, Diffusion-controlled mass transfer from a rotating cylinder, Numerical Heat Transfer A 23 (1993) 303-318.

[3] M. Prudhomme and L. Robillard, Natural convection in an annular fluid layer rotating at weak angular velocity. In: Proc. 4th Int. Symp. on Transport Phenomena, Heat and Mass TransferSydney, N.S.W., 1991, p. 38.

[4] F. Ladeinde, Studies on thermal convection in self-gravitating and rotating horizontal cylinders in a vertical external gravity field. 1988).

[5] T.S. Lee, Numerical computation of fluid convection with air enclosed between the annuli of eccentric heated horizontal rotating cylinders, Computers and Fluids 21 (1992) 355-368.

[6] E. Abu-Nada, Z. Masoud and A. Hijazi, Natural convection heat transfer enhancement in horizontal concentric annuli using nanofluids, International Communications in Heat and Mass Transfer 35 (2008) 657-665.

[7] H.C. Brinkman, The viscosity of concentrated suspensions and solutions, Journal of Chemical Physics 20 (1952).

[8] R.L. Hamilton and O.K. Crosser, Thermal conductivity of heterogeneous two-component system, I&EC Fundamentals 1 (1962) 187-191.

[9] E. Abu-Nada, Effects of variable viscosity and thermal conductivity of Al_2O_3-water nanofluid on heat transfer enhancement in natural convection, International Journal of Heat and Fluid Flow 30 (2009) 679-690.

[10] M. Izadi, A. Behzadmehr and D. Jalali-Vahida, Numerical study of developing laminar forced convection of a nanofluid in an annulus, International Journal of Thermal Sciences 48 (2009) 2119-2129.

[11] M. Izadi, A. Behzadmehr and D. Jalali-Vahida, Numerical study of developing laminar forced convection of a nanofluid in an annulus, International Journal of Thermal Sciences 48 (2009) 2119-2129.

[12] N. Masoumi, N. Sohrabi and A. Behzadmehr, A new model for calculating the effective viscosity of nanofluids, Journal of Physics D: Applied Physics 42 (2009) 055501.

[13] C.H. Chon, K.D. Kihm, S.P. Lee and S.U.S. Choi, Empirical correlation finding the role of temperature and particle size for nanofluid (Al_2O_3) thermal conductivity enhancement, Applied Physics Letters 87 (2005) 1-3.

[14] E.E. Feldman, R.W. Hornbeck and J.F. Osterle, A numerical solution of developing temperature for laminar developing flow in eccentric annular ducts, International Journal of Heat and Mass Transfer 25 (1982) 243-253.

[15] N.H. Abu-Sitta, K. Khanafer, K. Vafai and A.M. Al-Amiri, Combined forced- and natural-convection heat transfer in horizontally counterrotating eccentric and concentric cylinders, Numerical Heat Transfer; Part A: Applications 51 (2007) 1167-1186.

[16] M.I. Char and Y.H. Hsu, Computation of buoyancy-driven flow in an eccentric centrifugal annulus with a non-orthogonal collocated finite volume algorithm, International Journal for Numerical Methods in Fluids 26 (1998) 323-343.

[17] J. Buongiorno, Convective transport in nanofluids, Journal of Heat Transfer 128 (2006) 240-250.

[18] S. Maiga, S.J. Palm, C.T. Nguyen, G. Roy and N. Galanis, Heat transfer enhancement by using nanofluids in forced convection flows, International Journal of Heat and Fluid Flow 26 (2005) 530-546.

[19] C.T. Nguyen, F. Desgranges, G. Roy, N. Galanis, T. Mare, S. Boucher and H. Angue Mintsa, Temperature and particle-size dependent viscosity data for water-based nanofluids - Hysteresis phenomenon, International Journal of Heat and Fluid Flow 28 (2007) 1492-1506.

[20] K. Khanafer and K. Vafai, A critical synthesis of thermophysical characteristics of nanofluids, International Journal of Heat and Mass Transfer 54 (2011) 4410-4428.

[21] A. Bejan, Convection Heat Transfer, John Wiley & Sons, 2003.

[22] T.H. Kuehn and R.J. Goldstein, An experimental and theoretical study of natural convection in the annulus between horizontal concentric cylinders, Journal of Fluid Mechanics 74 (1976) 695-719.

[23] J.S. Yoo, Mixed convection of air between two horizontal concentric cylinders with a cooled rotating outer cylinder, International Journal of Heat and Mass Transfer 41 (1998) 293-302.